

Locality and universality of quantum memory effects

B.-H. Liu,^{1,*} S. Wißmann,^{2,*} X.-M. Hu,¹ C. Zhang,¹ Y.-F. Huang,¹
C.-F. Li,^{1,†} G.-C. Guo,¹ A. Karlsson,³ J. Piilo,³ and H.-P. Breuer^{2,‡}

¹Key Laboratory of Quantum Information, University of Science and Technology of China, CAS, Hefei, 230026, China

²Physikalisches Institut, Universität Freiburg, Hermann-Herder-Straße 3, D-79104 Freiburg, Germany

³Turku Centre for Quantum Physics, Department of Physics and Astronomy,
University of Turku, FI-20014 Turun yliopisto, Finland

(Dated: March 19, 2014)

Recently, a series of different measures quantifying memory effects in the quantum dynamics of open systems has been proposed. Here, we derive a mathematical representation for the non-Markovianity measure based on the exchange of information between the open system and its environment which substantially simplifies its numerical and experimental determination, and fully reveals the locality and universality of non-Markovianity in the quantum state space. We further illustrate the application of this representation by means of an all-optical experiment which allows the measurement of the degree of memory effects in a photonic quantum process with high accuracy.

PACS numbers: 03.65.Yz, 42.50.-p, 03.67.-a

In recent years the problem of characterizing non-Markovian dynamics in the quantum regime has initiated an intense debate. A series of diverse definitions along with measures of quantum memory effects have been proposed, invoking many different mathematical and physical concepts and techniques. Examples are characterizations of non-Markovianity in terms of deviations from a Lindblad semigroup [1], of the divisibility of the dynamical map [2], of the dynamics of entanglement [2] and correlations [3] with an ancilla system, and of the Fisher information [4].

In this work we focus on the measure of non-Markovianity introduced in Refs. [5, 6] which defines non-Markovianity through the backflow of information from the environment to the open system. This information backflow is characterized by an increase of the distinguishability of time-evolved quantum states. The distinguishability of two quantum states ρ_1 and ρ_2 is quantified by their trace distance $\mathcal{D}(\rho_1, \rho_2) = \frac{1}{2} \text{Tr} |\rho_1 - \rho_2|$ [7–9]. We assume that the open system Hilbert spaces \mathcal{H} is finite dimensional. The corresponding space of physical states, represented by the convex set of positive operators with unit trace, will be denoted by $\mathcal{S}(\mathcal{H})$. We further assume that the time evolution of the open system can be described by a 1-parameter family Φ [10] of completely positive and trace preserving dynamical maps Φ_t , i.e. $\Phi = \{\Phi_t \mid 0 \leq t \leq T, \Phi_0 = I\}$. The non-Markovianity measure can then be defined as

$$\mathcal{N}(\Phi) = \max_{\rho_1 \perp \rho_2} \int_{\sigma > 0} dt \sigma(t, \rho_1, \rho_2), \quad (1)$$

where

$$\sigma(t, \rho_1, \rho_2) \equiv \frac{d}{dt} \mathcal{D}(\Phi_t(\rho_1), \Phi_t(\rho_2)) \quad (2)$$

denotes the time derivative of the trace distance between the pair of states at time t . In Eq. (1) the time integral is

extended over all time intervals in which this derivative is positive, and the maximum is taken over all pairs of orthogonal initial states $\rho_1 \perp \rho_2$. This measure for non-Markovianity was originally defined in [5] in terms of a maximization over all pairs of quantum states in $\mathcal{S}(\mathcal{H})$. However, as demonstrated in Ref. [11] the maximization can be restricted to pairs of orthogonal initial states. We recall that two quantum states ρ_1 and ρ_2 are said to be orthogonal if their supports, i.e. the subspaces spanned by their nonzero eigenvalues are orthogonal which is equivalent to $\mathcal{D}(\rho_1, \rho_2) = 1$ [9]. This implies that optimal state pairs exhibiting a maximal backflow of information during their time evolution are initially distinguishable with certainty, and thus represent a maximal initial information content.

Although the orthogonality of optimal states greatly simplifies the mathematical representation of the non-Markovianity measure, its determination still requires the maximization over pairs of quantum states. Here, we derive a much simpler representation for the measure which is particularly relevant for its experimental realization since it only requires a local maximization over single quantum states, the second state being an arbitrary fixed reference state taken from the interior of the state space. This representation will further be employed in an all-optical experimental setup for the measurement of the non-Markovianity of a photonic process.

To formulate our main theoretical result we first define $\mathring{\mathcal{S}}(\mathcal{H})$ to be the interior of the state space, i.e. the set of all quantum states ρ_0 for which there is an $\varepsilon > 0$ such that all Hermitian operators ρ with unit trace satisfying $\mathcal{D}(\rho, \rho_0) \leq \varepsilon$ belong to $\mathcal{S}(\mathcal{H})$. We further define

$$\mathcal{E}_0(\mathcal{H}) = \{A \mid A \neq 0, A = A^\dagger, \text{Tr } A = 0\} \quad (3)$$

to be the set of all nonzero, Hermitian and traceless operators on \mathcal{H} . Considering any fixed reference state $\rho_0 \in \mathring{\mathcal{S}}(\mathcal{H})$ we can now introduce a particular class of

subsets of the state space: A set $\partial U(\rho_0) \subset \mathcal{S}(\mathcal{H})$ not containing ρ_0 is called an enclosing surface of ρ_0 if and only if for any operator $A \in \mathcal{E}_0(\mathcal{H})$ there exists a real number $\lambda > 0$ such that

$$\rho_0 + \lambda A \in \partial U(\rho_0). \quad (4)$$

Note that by definition ρ_0 itself is not contained in $\partial U(\rho_0)$ and that the full set $\partial U(\rho_0)$ is part of the state space. It can be easily seen that any state from the interior of the state space has an enclosing surface. For example, since ρ_0 is an interior point of the state space there is an $\varepsilon > 0$ such that the set of states ρ defined by $\mathcal{D}(\rho, \rho_0) = \varepsilon$ represents a spherical enclosing surface with center ρ_0 . However, an enclosing surface $\partial U(\rho_0)$ can have an arbitrary geometrical shape, the only requirement being that it encloses the reference state in all directions of state space. An example is shown in Fig. 1(a). Using these definitions, we can now state our central result.

Theorem. Let $\rho_0 \in \mathring{\mathcal{S}}(\mathcal{H})$ be any fixed state of the interior of the state space and $\partial U(\rho_0)$ an arbitrary enclosing surface of ρ_0 . For any dynamical process Φ , the measure for quantum non-Markovianity defined by Eq. (1) is then given by

$$\mathcal{N}(\Phi) = \max_{\rho \in \partial U(\rho_0)} \int_{\bar{\sigma} > 0} dt \bar{\sigma}(t, \rho, \rho_0), \quad (5)$$

where

$$\bar{\sigma}(t, \rho, \rho_0) \equiv \frac{\frac{d}{dt} \mathcal{D}(\Phi_t(\rho), \Phi_t(\rho_0))}{\mathcal{D}(\rho, \rho_0)} \quad (6)$$

is the derivative of the trace distance at time t divided by the initial trace distance.

Proof. Let $\rho \in \partial U(\rho_0)$. Applying the Jordan-Hahn decomposition [9] to the operator $\rho - \rho_0$ one concludes that there exists an orthogonal pair of states ρ_1 and ρ_2 such that

$$\rho_1 - \rho_2 = \frac{\rho - \rho_0}{\mathcal{D}(\rho, \rho_0)}, \quad (7)$$

and, hence, we have

$$\mathcal{D}(\Phi_t(\rho_1), \Phi_t(\rho_2)) = \frac{\mathcal{D}(\Phi_t(\rho), \Phi_t(\rho_0))}{\mathcal{D}(\rho, \rho_0)}, \quad (8)$$

by the linearity of the dynamical maps and the homogeneity of the trace distance. This shows that $\sigma(t, \rho_1, \rho_2) = \bar{\sigma}(t, \rho, \rho_0)$. It follows that the right-hand side of Eq. (5) is smaller than or equal to $\mathcal{N}(\Phi)$ as defined by Eq. (1). Conversely, suppose ρ_1, ρ_2 are two orthogonal states. Since $\rho_1 - \rho_2 \in \mathcal{E}_0(\mathcal{H})$, there exists $\lambda > 0$ such that $\rho \equiv \rho_0 + \lambda(\rho_1 - \rho_2) \in \partial U(\rho_0)$, by definition of an enclosing surface. Thus, one obtains $\rho_1 - \rho_2 = (\rho - \rho_0)/\lambda$. Since $\rho_1 \perp \rho_2$ we find $\mathcal{D}(\rho, \rho_0)/\lambda = \mathcal{D}(\rho_1, \rho_2) = 1$ and, hence, $\lambda = \mathcal{D}(\rho, \rho_0)$. Thus, we are again led to Eq. (7) and to $\sigma(t, \rho_1, \rho_2) = \bar{\sigma}(t, \rho, \rho_0)$. This shows that the measure $\mathcal{N}(\Phi)$ as defined by Eq. (1) is smaller than or equal

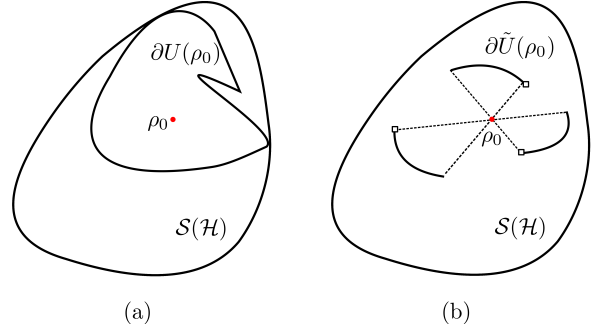


FIG. 1: (Color online) Illustration of an enclosing surface $\partial U(\rho_0)$ (a) and of a hemispherical enclosing surface $\partial \tilde{U}(\rho_0)$ with disconnected boundary (b) for an interior point ρ_0 of the state space $\mathcal{S}(\mathcal{H})$.

to the right-hand side of Eq. (5) which thus concludes the proof.

The theorem bears several important mathematical and physical consequences. First, it demonstrates that the non-Markovianity measure can be determined by maximization over single quantum states ρ taken from an arbitrary neighborhood of a fixed state ρ_0 in the interior of the state space. Thus, Eq. (5) provides a *local* representation of non-Markovianity, showing that quantum memory effects can be detected locally by sampling single states from an arbitrary enclosing surface of a fixed reference state. Note that the theorem cannot be applied to infinite dimensional Hilbert spaces since $\mathring{\mathcal{S}}(\mathcal{H})$ is empty in this case.

Second, the choice of the fixed reference state ρ_0 is completely arbitrary, the only condition being that it belongs to the interior of the state space. Thus, the non-Markovianity of a dynamical process is indeed a *universal* feature which appears everywhere in state space: The information about non-Markovian behavior is contained in any part of the state space which supports the intuitive idea that quantum memory effects represent an intrinsic property of the dynamical process. This fact is particularly relevant when dealing with a dynamical process that has an invariant state in the interior of the state space. It is then of great advantage to choose ρ_0 as this invariant state such that only the sampled states $\rho \in \partial U(\rho_0)$ evolve nontrivially in time.

Third, the theorem greatly simplifies the analytical, numerical or experimental determination of the non-Markovianity measure. In particular, it shows that it is not necessary to scan the whole state space in order to find an optimal pair of quantum states but rather sample the states of an enclosing surface of a fixed interior point of the state space. From the proof of the theorem we also see that it suffices if the enclosing surface contains all directions emanating from the fixed reference state ρ_0 exactly once, i.e. if Eq. (4) holds for exactly one $\lambda > 0$. It is even sufficient if this equation holds for either A or

–A. Therefore, the theorem is also valid if $\partial U(\rho_0)$ is replaced by a hemispherical enclosing surface $\partial \tilde{U}(\rho_0)$ which we define as follows. A set $\partial \tilde{U}(\rho_0) \subset \mathcal{S}(\mathcal{H})$ is said to be a hemispherical enclosing surface of ρ_0 if and only if for any $A \in \mathcal{E}_0(\mathcal{H})$ there exists exactly one real number $\lambda > 0$ such that either $\rho_0 + \lambda A \in \partial \tilde{U}(\rho_0)$ or $\rho_0 - \lambda A \in \partial \tilde{U}(\rho_0)$. A hemispherical enclosing surface thus contains all directions, given by operators $A \in \mathcal{E}_0(\mathcal{H})$, only once. Moreover, it needs neither be smooth nor connected (see Fig. 1(b) for an example) which makes this characterization particularly useful for noisy experiments.

We have applied the above theorem to determine the degree of non-Markovianity in a photonic process. The open quantum system is provided by the polarization degree of freedom of photons coupled to the frequency degree representing the environment. The experimental setup is depicted in Fig. 2. With the help of a frequency doubler a mode-locked Ti:sapphire laser (central wavelength 780 nm) is used to pump two 1 mm thick BBO crystals to generate the maximally entangled two-qubit state $(|H, V\rangle - |V, H\rangle)/\sqrt{2}$ with $|H\rangle$ and $|V\rangle$ denoting the horizontal and vertical polarization states, respectively [12]. A fused silica plate (0.1 mm thick and coated with a partial reflecting coating, with approximately 80 % reflectivity at 780 nm) serves as a Fabry-Pérot cavity (FP) which in addition can be tilted to generate different dynamical behavior [13]. The cavity and a consecutively placed interference filter (IF) (FWHM about 3 nm) single out two peaks near 780 nm of width $\sigma = 7.7 \times 10^{11}$ Hz each which are separated by $\Delta\omega = 7.2 \times 10^{12}$ Hz. The relative amplitude A_α of the two peaks depends strongly on the tilt angle α whereas the other quantities are almost constant. A polarizing beamsplitter (PBS) together with a half-wave plate (HWP) and a quarter-wave plate (QWP) are used as a photon state analyzer [14].

Photon 1 is directly detected in a single photon detector at the end of arm 1 as a trigger for photon 2. The optical setup in part *a*, *b* and *c* (see Fig. 2) is used to prepare arbitrary quantum states of photon 2 needed for the sampling process [15]. This set-up conveniently allows to prepare any single pure photon polarization state (in arm 2*c*) and reference states (2*a* along with 2*b*) together with arbitrary enclosing surfaces which can be controlled by changing the relative amplitudes of the attenuators built in in each arm. The path difference between each arm is about 25 mm to ensure that the mixture of the three parts is classical.

After the preparation photon 2 passes through birefringent quartz plates of variable thickness which couple the polarization and frequency degree of freedom and lead to the decoherence of superpositions of polarization states. The birefringence is given by $\Delta n = 8.9 \times 10^{-3}$ at 780 nm. The thickness of the quartz plates simulating different evolution times ranges from 75λ to 318λ in units of the central wavelength of the FP cavity.

Employing the Bloch vector representation, the set of

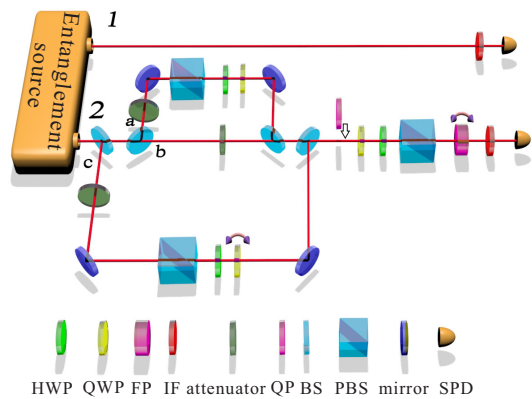


FIG. 2: (Color online) Experimental setup. Key to the components: HWP – half-wave plate, QWP – quarter-wave plate, FP – Fabry-Pérot cavity, IF – interference filter, QP – quartz plate, (P)BS – (polarizing) beam-splitter, SPD – single photon detector.

polarization states can be conveniently parametrized by means of spherical coordinates $\mathbf{r} = (r, \theta, \phi)$. We apply the local representation to two reference states to determine experimentally the degree of non-Markovianity for three dynamics characterized by the relative amplitudes $A_\alpha = 0.64, 0.22$ and 0.01 , ranging from non-Markovian to Markovian evolutions, and compare the results with the outcome for pairs of orthogonal initial states. The reference states ρ_0^1 and ρ_0^2 used in the experiment are given by

$$\mathbf{r}_0^1 = (0.20, \frac{1}{2}\pi, \frac{13}{50}\pi), \quad \mathbf{r}_0^2 = (0.88, \frac{8}{50}\pi, \frac{13}{50}\pi). \quad (9)$$

Reference state ρ_0^1 is thus located inside the equatorial plane, whereas the second reference state lies in the northern hemisphere close to the boundary. The enclosing surfaces are determined by the convex combination $0.3 \cdot \rho_0^{a,b} + 0.7 \cdot \rho$ of the reference states and any pure state prepared in arm 2*c*. These sets thus contain only mixed states. We measured a total of 5000 states on the surface for each reference state which are characterized by the azimuthal and polar angles of the pure states. The associated angles θ and ϕ are located on a lattice with equal spacing of $2\pi/100$.

The outcomes of the measurements are presented in Figs. 3, 4 and 5. The increase of the trace distance between 175λ and 318λ for any state on the enclosing surface for the two reference states is shown in Figs. 3(a)-5(a) and 3(b)-5(b) using color coding. Note, that the colored surfaces in these figures are non-spherical and not centered at the origin. By contrast, the ordinary Bloch spheres depicted in Figs. 3(c)-5(c) show the measurement outcomes for pairs of orthogonal initial states.

Defining spherical coordinates $\mathbf{r}_{\text{loc}} = (r_{\text{loc}}, \theta_{\text{loc}}, \phi_{\text{loc}})$ with respect to local coordinate systems centered at the position of the two reference states ρ_0^1 and ρ_0^2 , one recovers the polar symmetry present for pairs of orthogonal

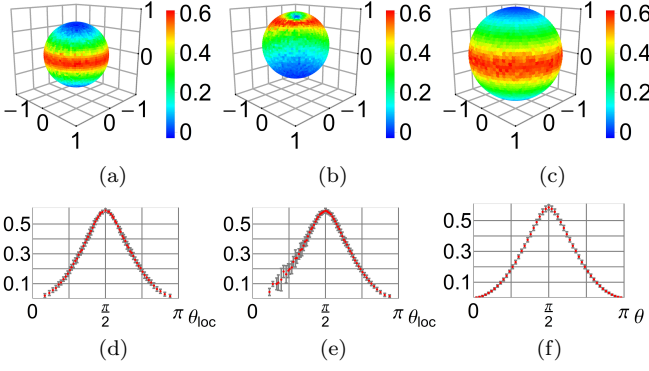


FIG. 3: (Color online) Experimental results for the increase of the trace distance between 175λ and 318λ for $A_\alpha = 0.64$ for states on the enclosing surface of reference state ρ_0^1 (a), ρ_0^2 (b) and pairs of orthogonal states (c). The corresponding ϕ_{loc} -averaged increase with respect to local spherical coordinates is shown in (d), (e) and (f). Error bars show the standard deviations.

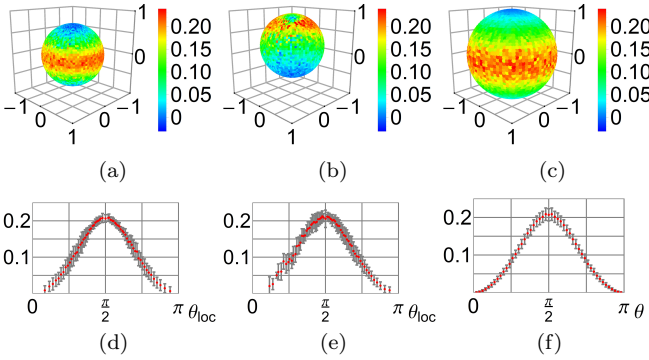


FIG. 4: (Color online) The same as Fig. 3 for $A_\alpha = 0.22$.

states, see Figs. 3(a)-(c). One may therefore average the outcomes over the polar angle ϕ_{loc} along lines of latitude. To this end, we introduced an appropriate binning on the z -axis and determined the average increase which we then assigned to the azimuthal angle θ_{loc} associated to the mean z -value in the bin. In addition, we allocated the standard deviation to each of the averaged outcomes. The resulting data are depicted in Figs. 3(d)-5(d) and 3(e)-5(e) and show the same characteristics as the ϕ -averaged increase of pairs of orthogonal states displayed in Figs. 3(f)-5(f). Note that the directional dependence of the trace distance originating from its property of depending only on the difference of two states can be nicely seen for example in Figs. 3(d)-(f).

The maximal increase of the trace distance for the two reference states obtained from the ϕ_{loc} -averaged data as well as for pairs of orthogonal states are given in Tab. I. The experimentally determined values are in very good

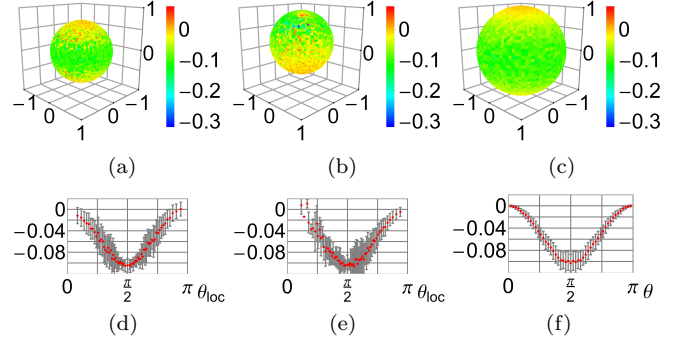


FIG. 5: (Color online) The same as Fig. 3 for $A_\alpha = 0.01$.

agreement with the predictions of the theoretical model [13], demonstrating the experimental feasibility and the accuracy of the method based on the local representation (5).

Summarizing, we have derived a representation of the measure for quantum non-Markovianity which fully reveals the locality and the universality of this measure. These properties are clearly reflected in the results of our photonic experiment. The experiment illustrates that the measure can be obtained efficiently in an arbitrary neighborhood of any fixed state in the interior of the state space, that its determination only requires a maximization over a single input state, and that optimal quantum states featuring maximal backflow of information can always be represented by mixed states.

A_α	$\mathcal{N}_{\text{theo}}$	$\mathcal{N}_{(a)}$	$\mathcal{N}_{(b)}$	$\mathcal{N}_{(c)}$
0.64	0.59	0.59 ± 0.01	0.59 ± 0.02	0.59 ± 0.02
0.22	0.21	0.21 ± 0.01	0.21 ± 0.02	0.21 ± 0.02
0.01	0	0.001 ± 0.013	-0.005 ± 0.008	-0.0002 ± 0.0015

TABLE I: The quantum non-Markovianity measure for the three dynamics obtained from the experimental data in comparison to the theoretical value.

This work was supported by the National Basic Research Program of China (2011CB921200), the CAS, the National Natural Science Foundation of China (11274289, 11325419, 11374288, 11104261, 61327901), the National Science Fund for Distinguished Young Scholars (61225025), the Fundamental Research Funds for the Central Universities (WK2470000011), the Academy of Finland (Project 259827), the Jenny and Antti Wihuri Foundation, the Magnus Ehrnrooth Foundation, and the German Academic Exchange Service (DAAD). S. W. thanks the German National Academic Foundation for support.

* These authors contributed equally to this work.

† cffi@ustc.edu.cn

‡ breuer@physik.uni-freiburg.de

- [1] M. M. Wolf, J. Eisert, T. S. Cubitt, J. I. Cirac, Phys. Rev. Lett. **101**, 150402 (2008).
- [2] A. Rivas, S. F. Huelga, and M. B. Plenio, Phys. Rev. Lett. **105**, 050403 (2010).
- [3] S. Luo, S. Fu, and H. Song, Phys. Rev. A **86**, 044101 (2012).
- [4] X.-M. Lu, X. Wang, C.P. Sun, Phys. Rev. A **82**, 042103 (2010).
- [5] H.-P. Breuer, E.-M. Laine, and J. Piilo, Phys. Rev. Lett. **103**, 210401 (2009).
- [6] E.-M. Laine, J. Piilo, and H.-P. Breuer, Phys. Rev. A **81**, 062115 (2010).
- [7] C. A. Fuchs and J. van de Graaf, IEEE Transactions on Information Theory **45**, 1216 (1999).
- [8] M. Hayashi, *Quantum Information* (Springer-Verlag, Berlin, 2006).
- [9] M. A. Nielsen and I. L. Chuang, *Quantum Computation and Quantum Information* (Cambridge University Press, Cambridge, 2000).
- [10] H.-P. Breuer and F. Petruccione, *The Theory of Open Quantum Systems* (Oxford University Press, Oxford, 2007).
- [11] S. Wißmann, A. Karlsson, E.-M. Laine, J. Piilo and H.-P. Breuer, Phys. Rev. A **86**, 062108 (2012).
- [12] X. L. Niu, Y. F. Huang, G. Y. Xiang, G. C. Guo and Z. Y. Ou, Optics Letters **33**, 968 (2008).
- [13] B.-H. Liu, L. Li, Y.-F. Huang, C.-F. Li, G.-C. Guo, E.-M. Laine, H.-P. Breuer, and J. Piilo, Nature Physics **7**, 931-934 (2011).
- [14] D. F. V. James, P. G. Kwiat, W. J. Munro and A. G. White, Phys. Rev. A **64**, 052312 (2001).
- [15] P. G. Kwiat, E. Waks, A. G. White, I. Appelbaum and P. H. Eberhard, Phys. Rev. A **60**, R775 (1999).